CASTOR, a new instrument for combined XRR-GIXRF analysis at SOLEIL

Yves Ménesguen, Bruno Boyer, H. Rotella, J. Lubeck, J. Weser, B. Beckhoff, D. Grötzsch, B. Kanngiesser, A. Novikova, E. Nolot, et al.

Special issue article

X-RAY SPECTROMETRY

Received: 31 August 2016 Revised: 28 November 2016 Accepted: 30 November 2016 Published online in Wiley Online Library: 13 January 2017

(wileyonlinelibrary.com) DOI 10.1002/xrs.2742

CASTOR, a new instrument for combined XRR-GIXRF analysis at SOLEIL

Y. Ménesguen,[a]* B. Boyer,[a] H. Rotella,[d] J. Lubeck,[b] J. Weser,[b] B. Beckhoff,[b] D. Grötzsch,[c] B. Kanngießer,[c] A. Novikova,[a] E. Nolot[d] and M.-C. Lépy[a]

A new instrument called CASTOR is operated at the SOLEIL synchrotron facility and is dedicated to the characterization of thin films with thicknesses in the nanometer range. The instrument can combine X-ray reflectivity measurements with fluorescence (XRF) acquisitions and especially total reflection X-ray fluorescence-related techniques such as grazing incidence XRF. The instrument was successfully installed and operated on the two branches of the metrology beamline making possible experiments over a wide range of photon energies (45 eV to 40 keV). A heating sample holder was developed to allow the sample temperature to be controlled up to 300° C. Some examples of the first studies are given to illustrate the capabilities of the setup.

Introduction

The characterization of multilayered thin-film structures with layer thicknesses in the nanometer range is commonly studied by X-ray reflectometry (XRR) on synchrotron facilities or with in-lab sources for years [1]. Reflectivity curves are acquired by varying the incident angle in the grazing incidence regime while recording the intensity of the specular-reflected beam. Grazing incidence X-ray fluorescence (GIXRF) is a total reflection X-ray fluorescence (XRF) analysis-related technique [2], which uses the XRF angle-dependent intensity at shallow incidence angles. The renewed interest for these techniques came from the elaboration of nanomaterials for applications in power electronics, electricity storage, and microelectronics, which require new means of characterization. The XRF signal is element-specific and contains information about the elemental composition, concentration profiles, and thicknesses. The combination of XRR, more sensitive to the atomic density, and GIXRF, sensitive to element density, produces results of better accuracy compared with one technique alone. Some experimental facilities have already been developed to allow GIXRF-XRR combined analysis, using either synchrotron radiation [3,4] or laboratory X-ray sources [5,6].

The Laboratoire National Henri Becquerel (LNHB) acquired an instrument to perform such measurements at the metrology beamline of the SOLEIL synchrotron source in order to propose metrological studies of thin-film deposits to support the efforts of institutes or companies in the fast-developing field of nanolayered structures. The instrument CASTOR (Chambre d'Analyse Spectrométrique en Transmission ou en Réflexion) is a seven-axis goniometer based on the model developed at the PTB and TU, Berlin [3,7]. Several differences exist with the first designed instrument. In particular, the plane of investigation of the sample is vertical and cannot be changed to horizontal, which means that the polarization of investigation is dependent on the source polarization. At the metrology beamline, the polarization is horizontal; the experiments will therefore be performed with P-polarization. This work describes the main part of the instrument and additional equipment, the experimental conditions at the metrology beamline of the SOLEIL synchrotron facility, and the first results obtained on selected samples.

Characteristics of the CASTOR apparatus

A compact design for a removable setup

The definition of the goniometer characteristics includes several aspects, from the number of independent axes, the performance and range of the motors, and the detectors to practical aspects related to the room available at the metrology beamline and security aspects. The height of the chamber is adjustable to adapt to the two branches of the metrology beamline (1420 mm on monochromatized hard X-ray and 1727 mm on the XUV branch). The chamber is aligned in the horizontal plane by a motorized translation stage perpendicular to the beam direction. The base frame has external dimensions of 840 × 840 mm on the floor, and the high-vacuum chamber has an inner diameter of 500 mm and an inner height of 700 mm. The chamber is equipped with a turbomolecular pump and the internal pressure can reach 10^{-5} Pa. Even if the internal components could be outgassed, which would allow even lower pressures, the room available and other practical aspects did not allow adding a load-lock chamber with a sample transfer system. Instead, the chamber is equipped with a fast-entry door on a DNCF160 flange, which would limit the

* *Correspondence to: Y. Ménesguen, CEA, LIST, Laboratoire National Henri Becquerel (LNE-LNHB), 91191 Gif-sur-Yvette cedex, France. E-mail: yves.menesguen@cea.fr*

Presented at EXRS2016 - European Conference on X-ray Spectrometry, Gothenburg, Sweden, 19-24 June 2016.

a *CEA, LIST, Laboratoire National Henri Becquerel (LNE-LNHB), 91191 Gif-sur-Yvette cedex, France*

b *Physikalisch-Technische Bundesanstalt, Abbestr. 2-12, 10587 Berlin,Germany*

c *Institut für Optik und Atomare Physik, Technische Universität Berlin, Hardenbergstr. 36, 10623 Berlin, Germany*

d *CEA, LETI, MINATEC, 17 rue des Martyrs, 38054 Grenoble cedex 9, France*

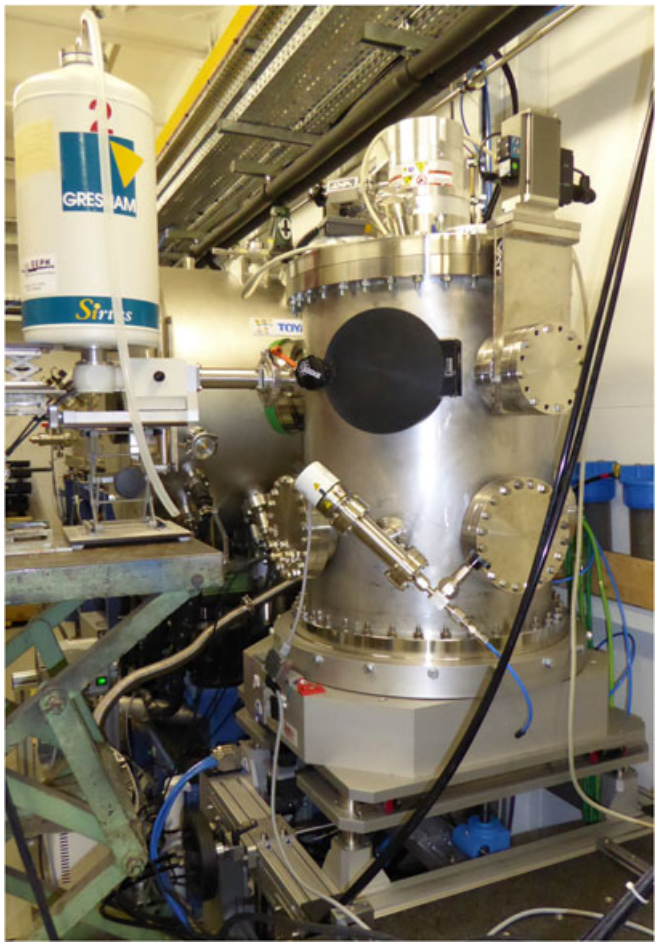

Figure 1. External view of the end-station CASTOR installed at the hard X-ray beamline.

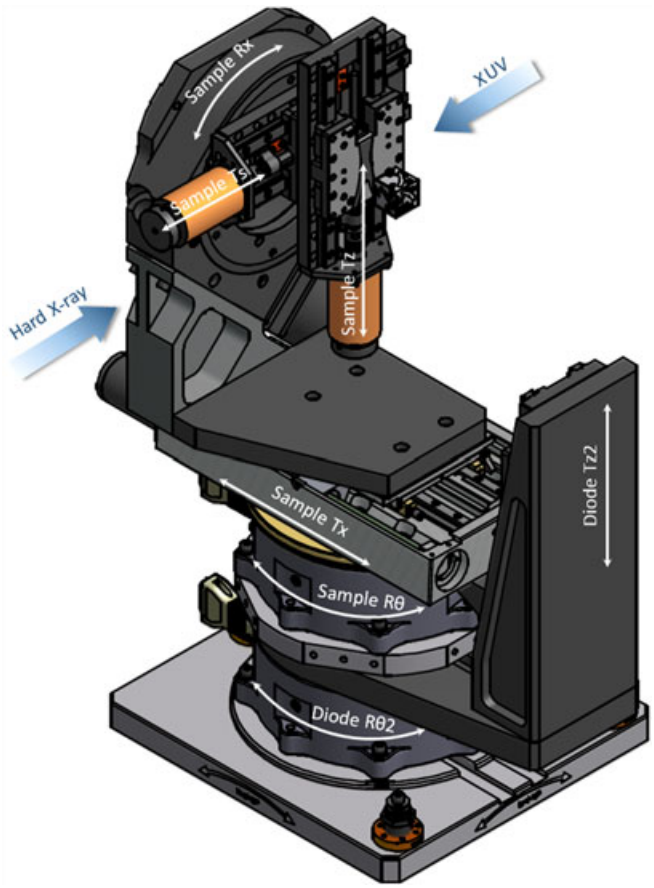

Figure 2. A schematic representation of the seven-axis goniometer. The beam may enter from either the right (XUV branch) or from the left (hard X-ray branch).

studies to samples that are temporarily exposed to air. As a consequence, the sample preparation conditions in the absence of a clean room will limit the achievable performance of surface contamination studies. Several flanges allow the motors, detectors, and vacuum gauges to be connected, and windows are placed to allow visual inspection of the chamber contents (Fig. 1).

Characteristics of the goniometer

The internal manipulator of CASTOR is composed of seven axes with five motors for the sample and two dedicated to the detection arm (Fig. 2). The samples are placed vertically on two perpendicular translation stages (namely Tz and Ts), which are mounted on a rotation stage (Rx). This three-axis platform is attached on a horizontal translation stage (Tx), which is on the upper rotation stage (Rθ). The detection arm is on a second rotation stage (Rθ2). The fourth translation (Tz2) allows the detector to be selected. The Rθ and Rθ2 are the most critical axes for the experiments and are encoded for better accuracy. They can rotate freely except that collisions are prevented by a limit switch on the Rθ arm. This configuration allows the sample manipulator and the detector arm to rotate freely within the chamber, a basic requirement because the photon beam may come from either the left or the right of the chamber. The rotation stage Rx has a range of 350°. The translation stages have 110 mm ranges except for Tx, which is limited to 102 mm. The performance of the sample motors was tested at PTB and successfully met the specifications. The results are presented in Table 1.

The detection arm Rθ2 is equipped with four photodiodes and includes the possibility to install the front part of an energy-dispersive detector (e.g. silicon drift detector (SDD)). The four dedicated slots for the photodiodes accept either 12.5 or 7.5 mm width between their two pins to be compatible with the most commonly used commercial diodes. The photodiode holders can be equipped with commutable slits or collimators. The current configuration is composed of three 100 mm^2 photodiodes from Opto Diode [8,9] that have a typical efficiency of 0.27 A/W within the photon energy range available at the beamline. Moreover, the AXUV100G photodiode equipped with no slit was absolutely calibrated using a cryogenic electrical-substitution radiometer [10]. The two other diodes are an AXUV:Ti photodiode equipped with a cross slit of 300 μm (used for vertical or horizontal alignment) and an AXUV:Al photodiode equipped with a 300 μm vertical slit (used for alignment or measurements). The Al coating is necessary to prevent the infrared or visible light degrading the dark current or background, improving the dynamic range of the reflectivity curves. A spectrometer such as an energy-dispersive detector is needed to perform fluorescence-related measurements such as GIXRF. It can be installed on the chamber facing the sample (i.e. at 90° with respect to the incoming beam.). Experiments can be performed using either a high-purity germanium spectrometer from OXFORD Instruments (118 eV resolution at 5.9 keV) already

Table 1. Performance of the stepper motor axes of the manipulator

Axis	Max. distance	Resolution	Speed	Yaw	Pitch	Roll
Sample Tx	102.68 mm	0.0025 mm	0.2 mm·s^{-1}	0.004°	—	0.003°
Sample Ts	110.81 mm	0.0025 mm	0.2 mm·s^{-1}	0.014°	0.011°	0.001°
Sample Tz	111 mm	0.0025 mm	0.2 mm·s^{-1}	0.004°	0.013°	0.002°
Sample Rθ	190.09°	0.0005°	0.2° .s^{-1}			
Sample Rx	348.23°	0.0005°	0.4° .s^{-1}			
Diode Tz2	110.92 mm	0.0025 mm	0.2 mm·s^{-1}			
Diode Rθ2	186.24°	0.0005°	0.2°·s^{-1}			

available or an SDD from AMPTEK (125 eV resolution), which will soon be operational. Despite its better resolving power, the high-purity germanium detector is less practical to use because of its liquid nitrogen cooling tank and its slow signal processing that limits the count-rate. Thus, long acquisition times are necessary to obtain spectra with acceptable statistics. Moreover, it cannot approach very close to the sample (not less than 15 cm), because of its limited length. This has two consequences. First, it enlarges the field of view, which limits the accuracy of the results. Second, the counting statistics is reduced, which lengthen the experiment. Nevertheless, it has better quantum efficiency at high-photon energies often required for heavy elements. The SDD will be mounted on a dedicated translation stage allowing it to approach as close as possible to the sample.

Heating module

Some materials of interest for microelectronics have temperature-dependent properties, for example, chalcogenides that can change between vitreous and crystalline phase at specific temperatures. For this reason, performing XRR or combined XRR-GIXRF measurements at different temperature levels will provide more information. Within the frame of the EMPIR ENG53 ThinErgy program, LNHB initiated a collaboration with the French metrology institute, the Laboratoire National de Métrologie et d'Essais, to build a heating sample holder with a temperature controller. The heating module is capable of heating two samples of $\sim$ 20 $\times$ 40 mm^2 up to 300° C, and its compactness does not limit any motion of the goniometer. It is fastened with only one accessible screw making it easy to install or remove. First tests have been performed with the heating module, and the temperature was stable to within 1° C. Nevertheless, a small bias may remain between the temperature probe and the sample because of weak heat conduction between the holder plate and the sample. Moreover, another bias is still possible between the sample front face exposed to the beam and its back attached to the heating holder. An independent temperature controller might help to ensure the confidence in the sample surface temperature in the future. In the frame of a European metrology project, CEA-LETI provided samples, and first results were encouraging.

Measurement conditions at the metrology beamline of the SOLEIL synchrotron facility

The metrology beamline

The new French synchrotron SOLEIL, an acronym for 'Optimized Source of LURE Intermediary Energy Light', is a research center located near Paris. The synchrotron radiation is emitted by 2.75 GeV electrons that circulate in a storage ring of 354 m circumference. Twenty-nine beamlines (over 42 possible) are installed either on dipoles or insertion devices (undulator or wiggler) and are now operating. The most frequent mode is the top-up mode with a current of 450 mA delivered with a stability of better than 0.3%. The metrology beamline is situated on a bending magnet, and the corresponding photon source has a divergence of 8 mrad. The incident white beam is shaped by a first cooled diaphragm with motorized apertures to provide photons to the hard X-ray and XUV branches. The two branches together cover the energy range from 45 eV to 40 keV. The goniometer CASTOR can be installed on both the hard X-ray and the XUV branches.

The hard X-ray branch

The hard X-ray branch selects photons in the 100 eV to 40 keV energy range, and its main components are presented in Fig. 3. The acceptance is 1.7 mrad horizontally and 0.153 mrad vertically. A first collimating slit situated at 12.4 m from the source reduces the vertical beam divergence to improve the spectral resolution if necessary. The monochromator is situated at 21 m from the source and consists of three optical combinations to cover the whole energy range:

1. A double-crystal monochromator with plane Si (111) crystal for the higher energies: 3–40 keV;
2. A Ni-C multilayer mirror plus a variable-line spacing (VLS) plane grating (1800 lines/mm): 0.5–3 keV;
3. A Ni coated mirror plus a VLS plane grating (800 lines/mm) for the lower energies: 100–800 eV.

Two slits of four independent lips define the beam to a maximum of 48 $\times$ 4 mm^2. The typical flux is around 10^{10} photons/s for a photon energy of 10 keV in a 2 $\times$ 2 mm^2 area. The monochromatic beam is then delivered to the measurement position either in the so-called unfocused mode or in focused mode using two mirrors:

1. An elliptical mirror M1 vertically focuses the beam to the exit slits.
2. A bendable mirror M2 allows variation of the vertical focusing at the measurement position.

Two series of filters can be interposed to reduce the photon flux and/or to provide reference binding energies for the monochromator energy calibration. Finally, retracting the monochromator gives an access to the white beam.

The XUV branch

The main components of the XUV branch are presented in Fig. 4. Its acceptance is 2 mrad$\times$0.5 mrad. The energy selection is performed using several VLS gratings (75 300 and 1200 lines/mm) in combination with an order-sorter filter for photon energies below 900 eV. The order-sorter is composed of three mirrors used in

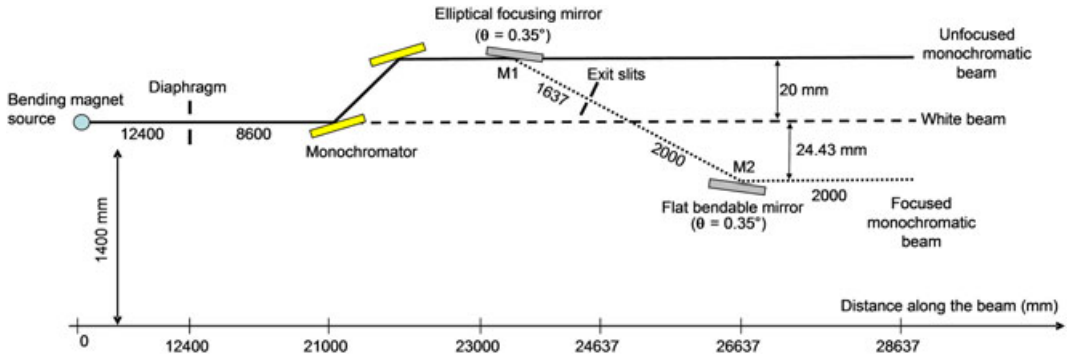

Figure 3. Metrology beamline at SOLEIL, the hard X-ray branch.

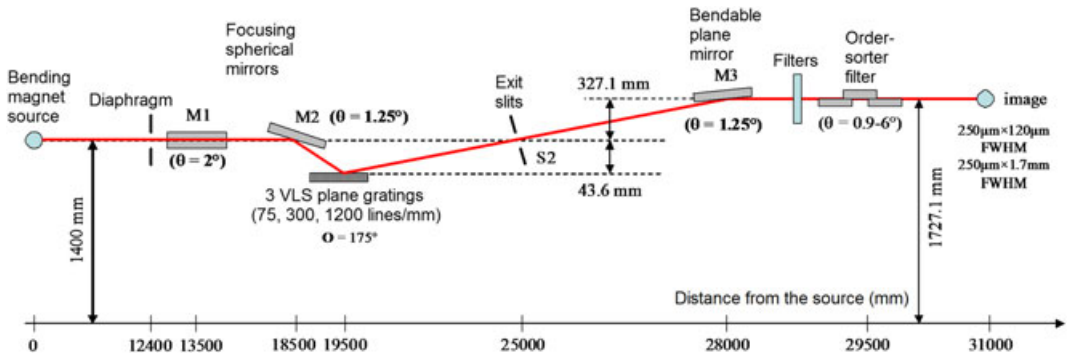

Figure 4. Metrology beamline at SOLEIL, the XUV branch.

grazing incidence (from 0.9–6°) with different coatings available to improve the efficiency of the order-sorter for different photon energy ranges:

1. The 75 lines/mm VLS plane grating: 45–300 eV;
2. The 300 lines/mm VLS plane grating: 300–1600 eV;
3. The 1200 lines/mm VLS plane grating: 900–1900 eV.

A series of thin filters are also available to help reduce the harmonics in some configurations. The beam size is approximately 250 μm width (full width at half maximum) and 120 μm height (full width at half maximum). At a photon energy of 1 keV, the flux can reach 10^{12} photons/s.

Performing data acquisition

A dedicated software for the instrument was developed by the LNHB. It runs under the LabVIEW® programming environment and uses the TANGO devices provided by SOLEIL to control all parameters. The program controls the vacuum, the motors, and the detectors, according to the SOLEIL command control requirements. Three measurement modes are possible: 'free run', 'reflectivity', and 'fluorescence'. The free-run mode does not allow recording any data. The photodiode current is measured repeatedly and plotted on a graph until the user stops it. The reflectivity mode allows the user to scan as many axes as desired with the possibility to record the photodiode current in an ASCII file. The fluorescence mode simultaneously acquires the photodiode current and a spectrum from the energy-dispersive detector, which is placed at 90° with respect to the incident beam. The spectra and the photodiode current are recorded in separate files using ASCII formats for both. In reflectivity mode as well as in the fluorescence mode, it is necessary to scan the two rotations Rθ and Rθ2 simultaneously in a linked mode, that is, $\theta 2 = 2 \times \theta$. A switch on the user interface binds the Rθ2 motion to the Rθ motion in order to measure the reflected beam with the photodiode at the correct position. All the motors can be scanned independently or in sequence. Some experiments require an energy scan instead of a position or the angle, and the program also allows scanning the photon energy provided by the beamline as for any other motor. This is of particular interest for X-ray absorption fine structure related techniques.

Examples of GIXRF and XRR as complementary techniques

Recent studies on a series of high-k materials prepared by CEA-LETI, which are of great interest for the semiconductor industry, were performed using the CASTOR set-up on the hard X-ray branch. The samples are ultra thin layer of Al_2O_3 high-k material deposited by atomic layer deposition technique on specific III-N based substrate. This substrate is a multilayered stack composed of GaN/buffer–AlGaN/AlN layers epitaxially grown on a Si substrate. The purpose of the stacking is to grow a good quality GaN layer on the Si substrate and thus adapt the crystal lattice mismatch. The thickness of the GaN top layer is large enough to be considered as the substrate with respect to grazing incidence fluorescence and reflectivity techniques. Considering the III-N devices, it is necessary to include a thin layer of AlGaN, before the dielectric layer, in order to produce the active transistor. As a consequence, the elemental profile of the Al and the Ga atoms, with respect to the depth, is required in order to assess the quality of the multilayered structure. XRR, combined with the GIXRF technique, allows the thickness, density, interface roughness, and

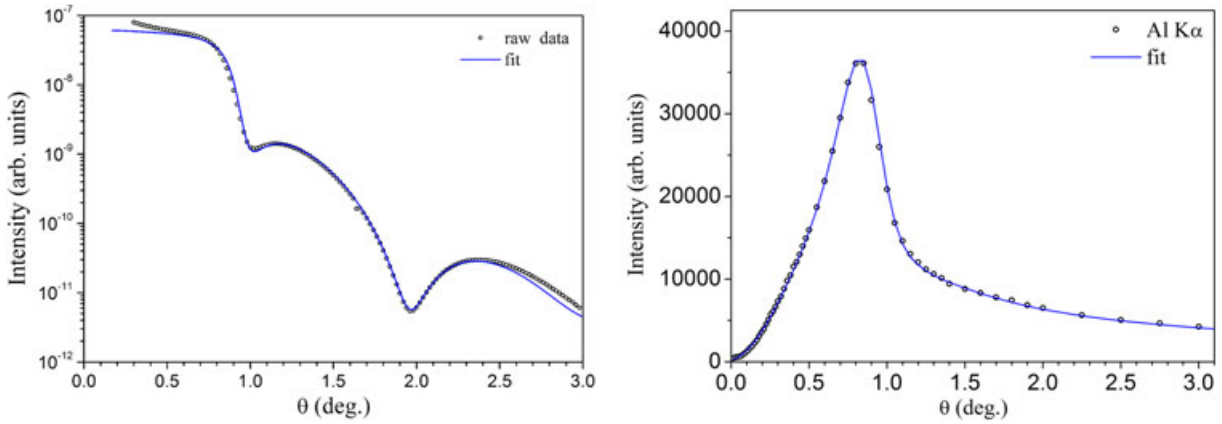

Figure 5. GIXRF-XRR performed at an excitation photon energy of 3 keV for the 10 nm Al_2O_3 layer on substrate. Left: XRR measurement and fit. Right: Angular dependence of the fluorescence intensity of the Al K_α line.

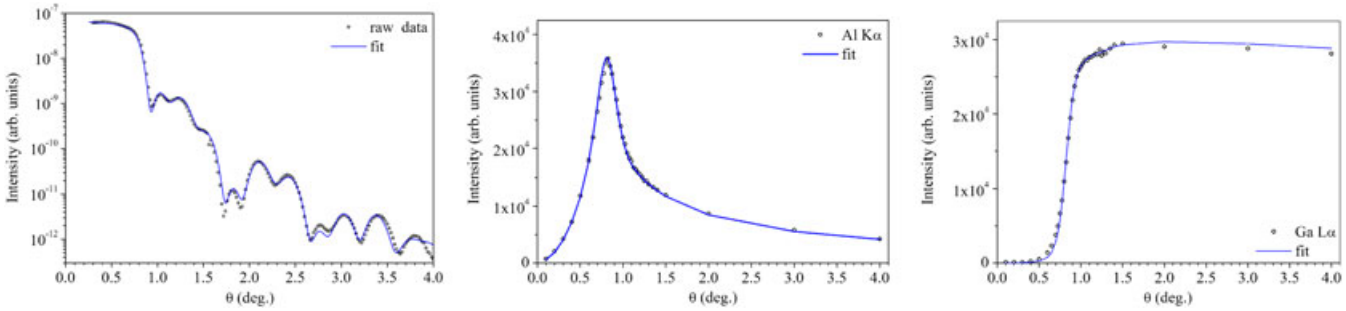

Figure 6. GIXRF-XRR performed at an excitation photon energy of 3 keV for the 10 nm Al_2O_3 layer on AlGaN. Left: XRR measurement and fit. Center and right: angular dependence of the fluorescence intensity of the Al K_α line and the Ga L_α lines, respectively.

Table 2. Results of the best fitting parameters for the two samples, using Leptos® software for XRR and the JGIXA software for the combined XRR-GIXRF analysis

Al^2O^3 nominal thickness	10 nm	10 nm on AlGaN
XRR	Al_2O_3: 9.8(8) nm; 3.1(1) g·cm^{-3}, roughness: 1.1(3) nm GaN substrate: 6.1 g·cm^{-3}, roughness: 0.6(3) nm	Al_2O_3: 10.9(3) nm; 3.0(1) g·cm^{-3}, roughness: 1.0(2) nm $Al_xGa_{1-x}N$: 25.2(9)nm; 5.1(2) g·cm^{-3},roughness: 0.7(3)nm, x=30.0% GaN substrate: 6.1 g·cm^{-3}, roughness: 0.0(2) nm
XRR-GIXRF	Al_2O_3: 9.81 nm; 3.15 g·cm^{-3}, roughness: 1.1 nm GaN substrate: 6.1 g·cm^{-3}, roughness: 0.3 nm	Al_2O_3: 11.05 nm; 3.21 g·cm^{-3}, roughness: 1.2 nm $Al_xGa_{1-x}N$: 25.06 nm; 5.11 g·cm^{-3}, roughness: 0.5 nm GaN substrate: 6.1 g·cm^{-3}, roughness: 0.5 nm

element diffusion to be determined. Here we performed the combined GIXRF-XRR analysis on both sample Al_2O_3/substrate and Al_2O_3/AlGaN/substrate. The Al_2O_3 layers are 10-nm thick, and the AlGaN layer is 25-nm thick. The measured and fitted XRR and GIXRF data acquired at an excitation energy of 3 keV on both samples are presented in Figs 5 and 6, respectively. First of all, we performed a preliminary analysis based only on the XRR data using the Leptos® software. Then, we performed a second analysis with the JGIXA software [11] including the fluorescence spectra to derive the aluminum K_α full-energy peak area with respect to the incident angle. The results of both analyses are shown in Table 2. Both analyses give similar results in terms of thickness, roughness, and density; however, the combined analysis provided the information that the elemental profile of aluminum is well represented by a model of two and three layers for both samples, respectively. Thus, we can conclude that the layers seem homogeneous without significant interfaces atomic diffusion. Nevertheless, we observe small discrepancies in the fit of the XRR data in Fig. 6 left, and further analysis is undergoing and will be presented later.

Conclusion

These first results underline the strong interest of the combined XRR-GIXRF analysis to measure the elemental profile of complex system with a non-destructive approach. Indeed, in semiconductor devices, the interface structure and the elemental distribution over the layers of the stack play a crucial role in the device performance. Thus, it is crucial to have an access to this information

in order to have a better insight of the device. Here we present a tool to a powerful non-destructive technique, which allows such characterization. CASTOR is a new instrument developed in collaboration between the metrological institutes PTB and LNHB that is installed on the Metrology beamline at the synchrotron SOLEIL in order to perform XRR in combination with GIXRF on multilayered thin-film samples that are of interest for a wide range of applications. The commissioning of the instrument established the performance of the motors, as well as the installation on the beamline including the achievement of the dedicated software and mechanical parts, customized diodes and spectrometer holders. The first results of the XRR-GIXRF combined technique obtained were successful, and optimizing the outcome with a full assessment of the uncertainties is an ongoing process. In the future, the LNHB will concentrate on the spectrometer response function/efficiency characterization, the management of the solid angle of detection when approaching the spectrometer towards the sample and data analysis using the dedicated software.

Acknowledgements

The authors are grateful to the European Metrology Research Program (EMRP) within the projects NEW01 TReND and ENG53 ThinErgy. 'The EMRP is jointly funded by the EMRP participating countries within EURAMET and the European Union'. The authors wish to thank Pascal Mercere and Paulo Da Silva for assistance on the metrology beamline and to the SOLEIL staff for smoothly running the facility and participating in the setup of the instrument on the Metrology beamline. The PTB and TU staffs are gratefully thanked for the conception of the instrument and the characterization of the motors. The LNE staff is gratefully thanked for the conception of the heating module.

References

[1] L. G. Parratt, Surface studies of solids by total reflection of X-Rays, *Physical Review* **1954**, *95*, 359–369.
[2] D. K. G. de Boer, Glancing-incidence x-ray fluorescence of layered materials, *Physical Review B* **1991**, *44*, 498–511.
[3] J. Lubeck, B. Beckhoff, R. Fliegauf, I. Holfelder, P. Hönicke, M. Müller, B. Pollakowski, F. Reinhardt, Weser, A novel instrument for quantitative nanoanalytics involving complementary x-ray methodologies, *Review of Scientific Instruments* **2013**, *84*, 045106.
[4] G. Das, S. R. Kane, A. Khooka, A. K. Singh, M. K. Tiwari, Simultaneous measurement of x-ray reflectivity and grazing incidence fluorescence at bl-16 beamline of indus-2, *Review of Scientific Instruments* **2015**, *86*, 055102.
[5] D. Ingerle, M. Schiebl, C. Streli, P. Wobrauschek, Combination of grazing incidence x-ray fluorescence with x-ray reflectivity in one table-top spectrometer for improved characterization of thin layer and implants on/in silicon wafers, *Review of Scientific Instruments* **2014**, *85*, 083110.
[6] M. Spanier, C. Herzog, D. Grötzsch, F. Kramer, I. Mantouvalou, J. Lubeck, J. Weser, C. Streeck, W. Malzer, B. Beckhoff, B. Kanngiesser, A flexible setup for angle-resolved X-ray fluorescence spectrometry with laboratory sources, *Review of Sc* **2016**, *87*, 035108.
[7] J Lubeck, M Bogovac, B Boyer, B Detlefs, D Eichert, R Fliegauf, D Grötzsch, I Holfelder, P Hönicke, W Jark, R. Kaiser, B Kanngießer, A. Karydas, J. Leani, M. Lépy, L Lühl, Y Ménesguen, A Migliori, M Müller, B Pollakowski, M Spanier, H Sghaier, G Ulm, J Weser, B Beckhoff, A new generation of x-ray spectrometry UHV instruments at the SR facilities BESSY II, ELETTRA and SOLEIL, in *AIP Conference Proceedings*, vol. 1741, AIP, New York, **2016**, pp. 030011.
[8] Opto Diode Corporation (US). [Online]. Available: http://optodiode.com/.
[9] R. Korde, C. Prince, D. Cunningham, R. E. Vest, E. Gullikson, Present status of radiometric quality silicon photodiodes, *Metrologia* **2003**, *40*, S145–S149.
[10] P Troussel, N Coron, BOLUX: a cryogenic electrical-substitution radiometer as high accuracy detector in the 150-11000 eV range, *Nuclear Instruments & Methods in Physics Research, Section A: Accelerators, Spectrometers, Detectors, and Associated Equipment* **2010**, *614*, 260–270.
[11] D. Ingerle, F. Meirer, G. Pepponi, E. Demenev, D. Giubertoni, P. Wobrauschek, C Streli, Combined evaluation of grazing incidence X-ray fluorescence and X-ray reflectivity data for improved profiling of ultra-shallow depth distributions, *Spectrochimica Acta, Part B: Atomic Spectroscopy* **2014**, *99*, 121–128.